

## Supplementary Information

### **Engineering the heart: Evaluation of conductive nanomaterials for improving implant integration and cardiac function**

Jin Zhou<sup>1, #</sup>, Jun Chen<sup>2, #</sup>, Hongyu Sun<sup>1, #</sup>, Xiaozhong Qiu<sup>3, #</sup>, Yongchao Mou<sup>1</sup>, Zhiqiang Liu<sup>1</sup>,  
Yuwei Zhao<sup>1</sup>, Xia Li<sup>1</sup>, Yao Han<sup>1</sup>, Cuimi Duan<sup>1</sup>, Rongyu Tang<sup>1</sup>, Chunlan Wang<sup>1</sup>, Wen Zhong<sup>4</sup>, Jie  
Liu<sup>5</sup>, Ying Luo<sup>5</sup>, Mengqiu Xing<sup>2, \*</sup>, Changyong Wang<sup>1, \*</sup>

<sup>1</sup>Department of Advanced Interdisciplinary Studies, Institute of Basic Medical Sciences and Tissue Engineering Research Center, 27 Taiping Rd, Academy of Military Medical Sciences, Beijing China.

<sup>2</sup>Department of Mechanical and Manufacturing Engineering, Faculty of Engineering, Department of Biochemistry and Medical Genetics, Faculty of Medicine, University of Manitoba and Manitoba Institute of Child Health, Winnipeg, Manitoba, Canada.

<sup>3</sup>Department of Anatomy, Southern Medical University, Guangzhou Guangdong, China.

<sup>4</sup>Department of Textile Sciences, Faculty of Human Ecology, Department of Medical Microbiology, Faculty of Medicine, University of Manitoba, Canada.

<sup>5</sup>Department of Biomedical Engineering, College of Engineering, 5 Yiheyuan Rd, Peking University, HaidianDist, Beijing, China.

## Contents

<b>1. Supplementary Figures</b> .....	<b>4</b>
<b>Figure S1. Gross morphology of SWNT/gelatin hydrogels (a) and gelatin hydrogels (b).</b>	
<b>Figure S2. Cytotoxicity assay.</b>	
<b>Figure S3. Assessment of cell proportions in c-ECTs on day 3 and 8.</b>	
<b>Figure S4. Evaluation of protein expression.</b>	
<b>Figure S5. Expression of cardiac proteins in g-ECTs and c-ECTs on day 8 with or without electrical stimulation.</b>	
<b>Figure S6. Gross morphology of c-ECTs and g-ECTs on infarcted areas after 4 weeks of implantation.</b>	
<b>Figure S7. Immunostaining of the boundary zone between c-ECTs and infarcted areas.</b>	
<b>Figure S8. CD68 immunostaining in g-ECTs, NCM and sham groups.</b>	
<b>Figure S9. FT-IR spectra analysis.</b>	
<b>Figure S10. Swelling capacity of SWNT/gelatin hydrogels.</b>	
<b>2. Supplementary Data</b> .....	<b>7</b>
<b>Fourier transforms infrared (FTIR) spectroscopy</b>	
<b>Swelling test</b>	
<b>3. Supplementary Tables</b> .....	<b>9</b>
<b>Supplementary table T1. Summary of the experimental outline.</b>	
<b>Supplementary table T2. Summary of echocardiography-data.</b>	
<b>Supplementary table T3. Summary of echocardiography-data.</b>	

4. **Supplementary Movies** .....10

**Supplementary Movie M1. Three dimensional live cell imaging of c-ECTs at day 8.**

**Supplementary Movie M2. Light microscope of synchronously contracted c-ECTs at day 8.**

**Supplementary Movie M3. Intracellular calcium transient measurement of c-ECTs under spontaneous condition.**

**Supplementary Movie M4. Intracellular calcium transient measurement of c-ECTs under point stimulation condition.**

5. **Supplementary Methods** .....11

**Scanning electron microscopy (SEM) analysis**

**Mechanical Testing**

**Electrical measurements**

**Cell viability assays**

**Construction of g-ECTs and Non-cardiomyocytes grafts**

**Cardiac patch labeling and 3-D live cell imaging**

**Histology and immunofluorescence *in vitro*.**

**Transmission electron microscopy analysis**

**Western blotting *in vitro***

**Intracellular calcium transient measurement**

**Histology and immunofluorescence *in vivo*.**

**Echocardiography**

**Left ventricular catheterization**

**Western blot analysis *in vivo***

## Supplementary Figures

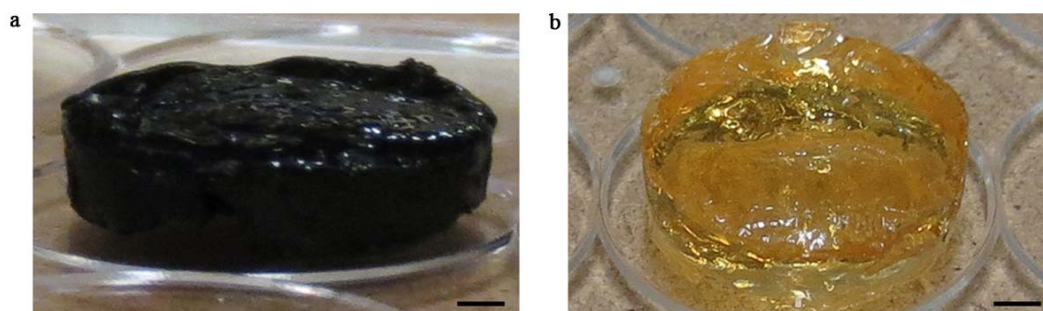


**Figure S1. Gross morphology of SWNT/gelatin hydrogels (a) and gelatin hydrogels (b). Scar bars=2mm.**

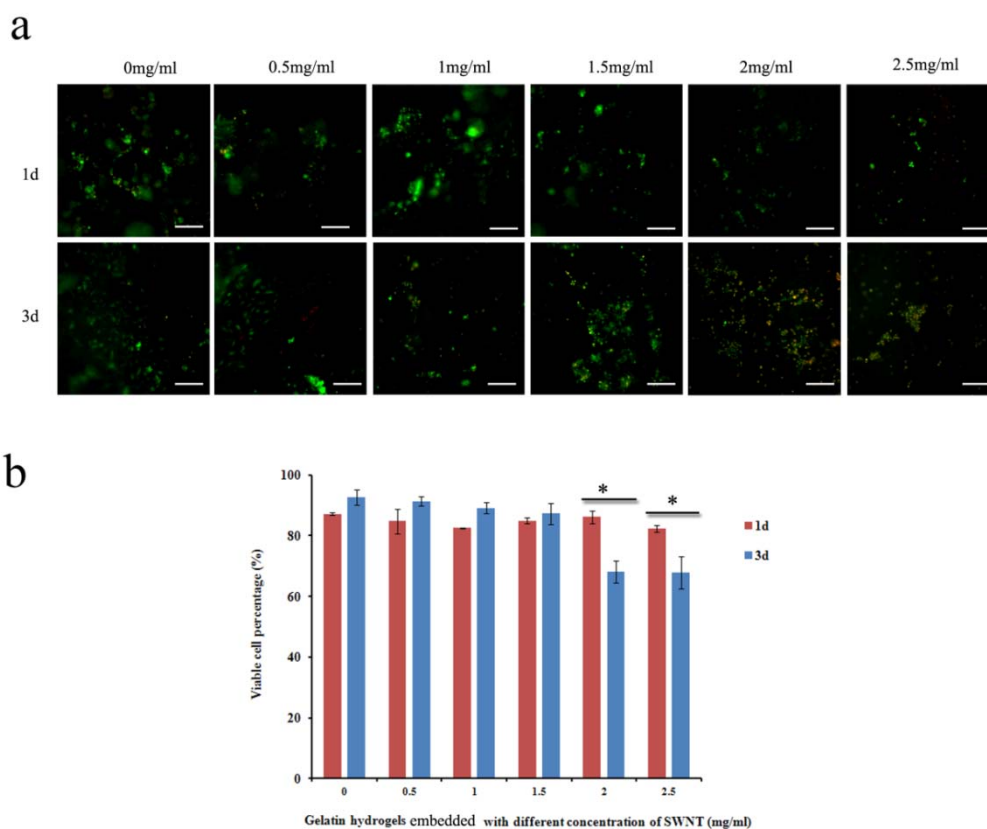


**Figure S2. Cytotoxicity assay.** Cell viability within the gelatin hydrogels embedded with different concentration of SWNTs (0, 0.5, 1, 1.5, 2 and 2.5mg/ml) was analyzed using Live/Dead Viability/Cytotoxicity assay at day 1 and day 3. Data are expressed

as mean  $\pm$  standard error of the mean (s.e.m.).  $n=6$  for each group. Scar bars=200 $\mu$ m.

Data are mean  $\pm$  s.e.m.  $*=p<0.05$ .

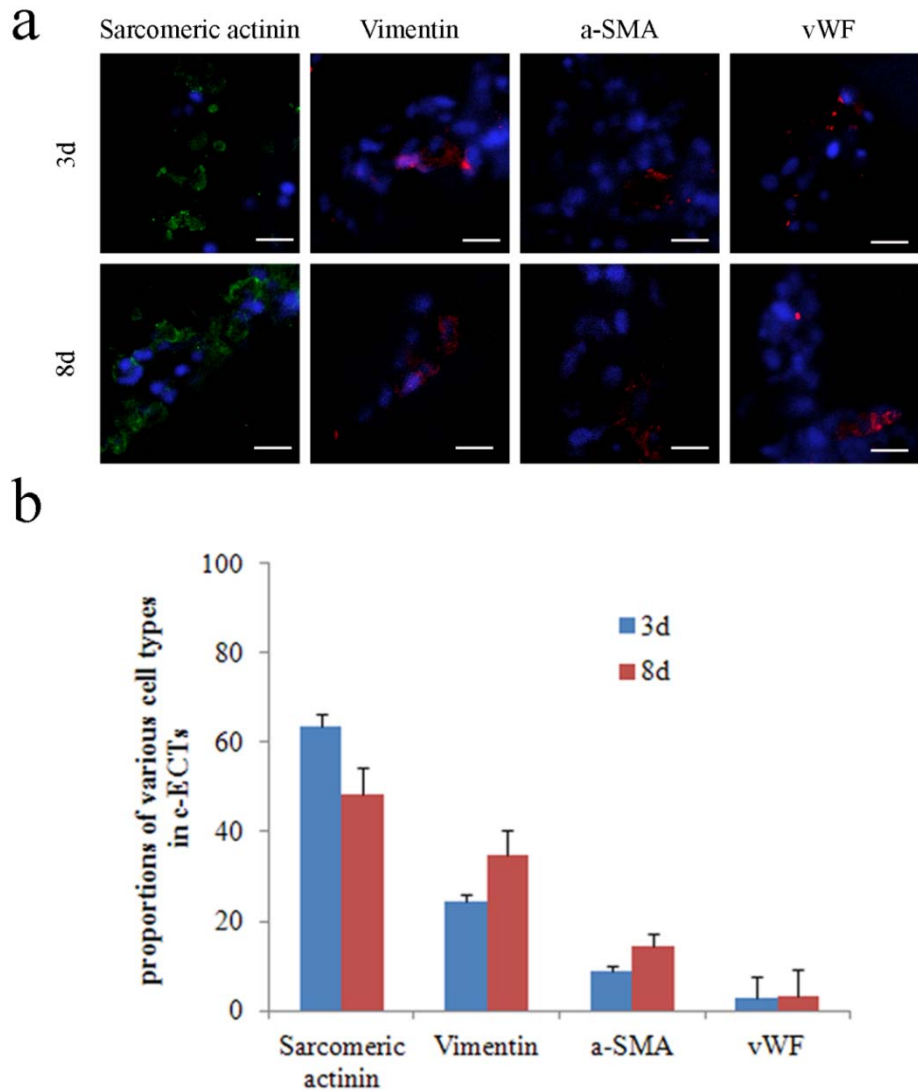


**Figure S3. Assessment of cell proportions in c-ECTs on day 3 and 8.** **a**, Various cell types in c-ECTs on day 3 and 8 were recognized based on their specific marker by immunofluorescence staining, such as the cardiomyocyte-specific marker sarcomeric actinin, the fibroblast marker vimentin, vascular smooth muscle cell marker a-SMA (alpha-smooth muscle actin) and the endothelial cell marker vWF (Von Willebrand

factor). b, Statistical analysis of various cell types in c-ECTs on day 3 and 8. n= 6 for each group. Nuclei were stained blue. Scar bars=20 $\mu$ m.

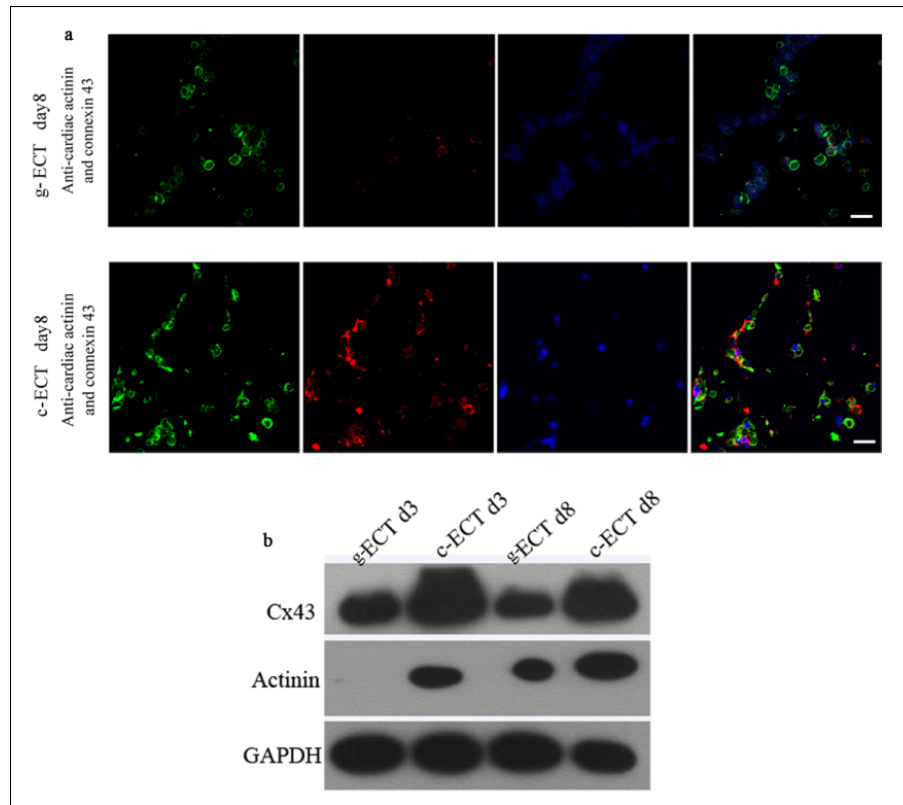


**Figure S4. Evaluation of protein expression.** a, Sarcomeric actinin (red) and Cx43 (green) double-immunostaining showed Cx43 expression strongly along cardiomyocytes in c-ECTs compared with low expressions in g-ECTs. Nuclei were stained blue. Scar bars=20 $\mu$ m. b, Representative western blot pictures of Cx43 and sarcomeric actinin expression on days 3 and 8.

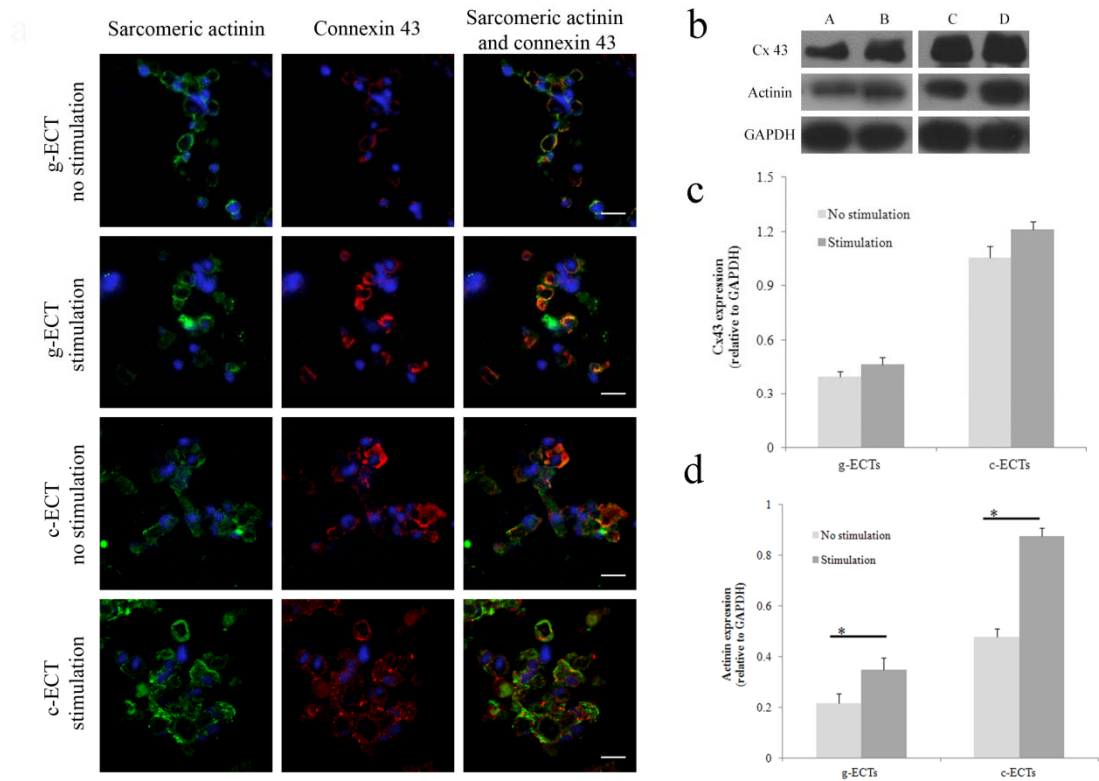


**Figure S5. Expression of cardiac proteins in g-ECTs and c-ECTs on day 8 with or without electrical stimulation. a,** Immunofluorescence staining of sarcomeric actinin (green) and cx43 (red) showed that cardiomyocytes in stimulated c-ECT exhibited strong expression of Cx43 between adjacent cells in contrast to expression of Cx43 along the cell plasmalemma in nonstimulated c-ECTs. Cardiomyocytes in nonstimulated or stimulated g-ECTs expressed relatively low levels of Cx43 along the cell plasmalemma. Scar bars=20 $\mu$ m. **b,** Western blot demonstrated that electrical stimulation elevated the levels of sarcomeric actinin in g-ECTs and c-ECTs on day 8 while the expression levels of Cx43 had not an obvious increase. A: nonstimulated g-ECTs; B: stimulated g-ECTs; C: nonstimulated c-ECTs; D: stimulated c-ECTs. **c,** Bar graphs showing quantification of the expression level of Cx43 compared with the expression of GAPDH in g-ECTs and c-ECTs on day 8 with or without electrical



stimulation. d, Bar graphs showing quantification of the expression level of sarcomeric actinin compared with the expression of GAPDH in g-ECTs and c-ECTs on day 8 with or without electrical stimulation. Data are mean  $\pm$  s.e.m.  $*=p<0.05$

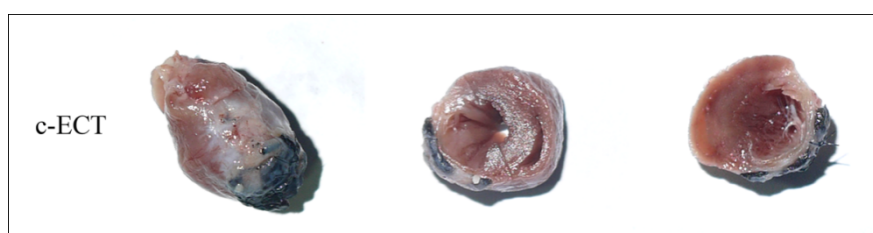


**Figure S6. Gross morphology of c-ECTs on infarcted areas after 4 weeks of implantation.**

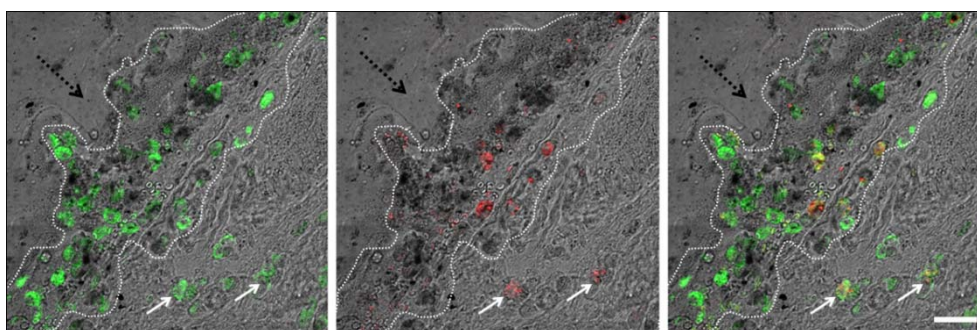


**Figure S7. Immunostaining of the boundary zone between c-ECTs and infarcted areas.** CD68 positive macrophages (green) migrated from the c-ECTs to the infarcted area, with apparent accumulation in the boundary zone and in scar areas. Some of these macrophages were c-ECTs-derived DiI<sup>+</sup> macrophages (red+ green). Nuclei were stained blue. Scar bars=20 $\mu$ m.

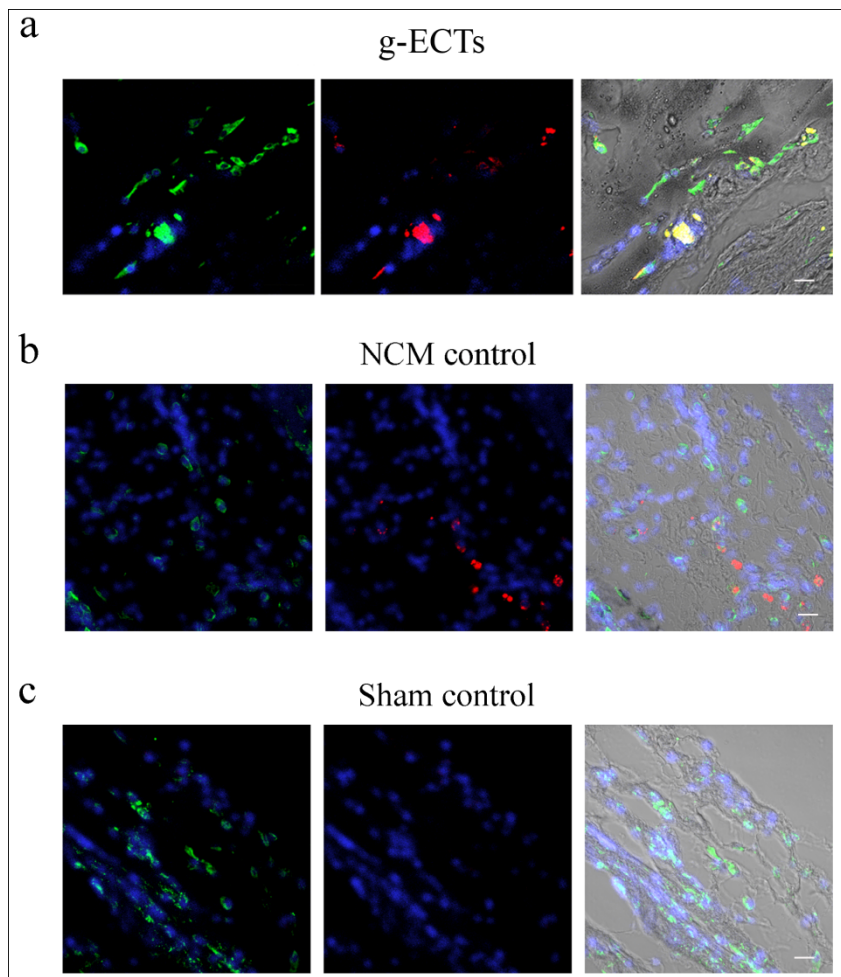


**Figure S8. CD68 immunostaining in g-ECTs, NCM and sham groups.** Some CD68 positive macrophages (green) could be detected within the scar areas of NCM and sham groups. Nuclei were stained blue. Scar bars=20 $\mu$ m.

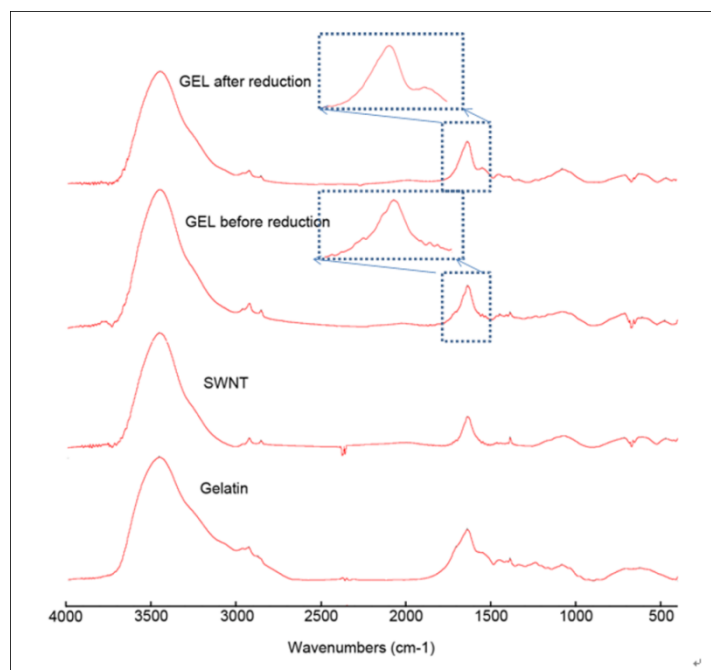


**Figure S9. FT-IR spectra analysis.** The FT-IR spectra of gelatin, single-wall carbon nanotubes, SWNT-gelatin hydrogels without reduction and gelatin hydrogels after reduction (all gelatin are 7.5 mg/mL in the gels).

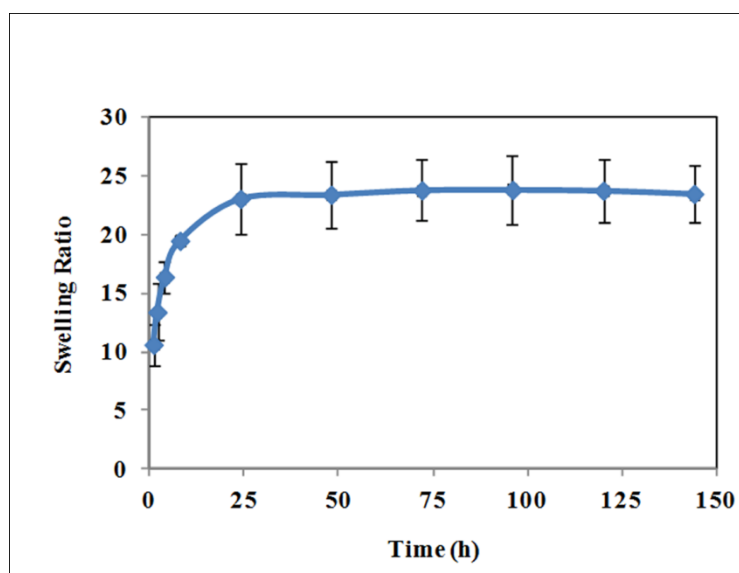


**Figure S10. Swelling capacity of SWNT/gelatin hydrogels.** The swelling ratio of SWNT (1.5 mg/mL)-gelatin (7.5 mg/mL) hydrogels at pH 7.4, room temperature as a function of time (h). n=3.

## Supplementary Data

### 1. Fourier transforms infrared (FTIR) spectroscopy

FTIR was used to characterize the gel formation. It was carried out as follows: the freeze-dried hydrogels were ground to powder, mixed with KBr, and compressed into KBr pellets. FTIR spectra were then recorded with a Thermo Scientific IR100 FT-IR Spectrometer. For single-wall carbon nanotubes, the typical C=O stretching absorption peak was found in the Supplementary Fig. S9, which was attributed to the COOH groups on the walls. After well-dispersed by the amphiphilic copolymer Pluronic F-127 in aqueous solutions, it was mixed with gelatin solutions to make the stock solutions. Then the cross-linker, glutaraldehyde was added to trigger the cross-linking reaction between the amino groups in the gelatin side chains to form the imine groups. As shown in the Fig. S7, the peak at around 1690  $\text{cm}^{-1}$  was attributed to the C=N stretching absorption, and the peak at around 1720  $\text{cm}^{-1}$  was attributed to the C=O stretching of aldehyde groups in mono-conjugated glutaraldehyde. After 30 min reaction, sodium cyanoborohydride was used to reduce the imine groups to C-N groups. At the same time, the excess of aldehyde groups in glutaraldehyde was consumed to distinguish the crosslinking reaction. The peaks at  $\sim 1690 \text{ cm}^{-1}$  and 1720  $\text{cm}^{-1}$  both disappeared, which suggested the reduction reaction successfully removed the imine groups and aldehyded groups, thus enhanced compatibility.

### 2. Swelling test

Dried hydrogels were placed in 5 mL of phosphate buffer at pH 7.4 at room temperature. Swollen hydrogels were weighed at 1, 2, 4, 8 h, 1, 2, 3, 4, 5 d, and 6 days

to characterize the swelling kinetics. The swelling weight ratio (SWR) at each time point was calculated as:  $SWR = (W_s - W_d) / W_d$ ; where  $W_s$  is the weight of the swollen gel (g) and  $W_d$  is the original weight of the dry gel (g).

The swelling ratio was determined to demonstrate the water content in the formed hydrogels. As shown in supplemental Fig. S10, after 1 h immersion, the hydrogels had the 10 fold weight in compared with the dried sample. And a rapid water absorption process was observed in the first day, which can reach ~ 22 fold weight of water absorption. And a plateau showed afterwards till 1 week. The fast swelling was believed due to the good hydrophilicity of gelatin and the swelling ratio of hydrogels showed a minimum decrease, which may indicate that the hydrogels was very stable in such condition (PBS, pH=7.4).

## Supplementary Tables

**Supplementary table 1: Summary of the experimental outline**

LAD ligation:	136			
Survived LAD ligation:	102			
Infarcted rats with FS <30%:	73			
Experiment of heart function	Experimental groups			
	Sham	c-ECT	g-ECT	NCM
Echocardiography	15	16	12	11
Catheterization	10	10	8	8
Experiment of carbon nanotubes transportation	Health 6	c-ECT 8		
Experiment of macrophages infiltration		g-ECT 6	c-ECT 6	

**Supplementary table 2: Summary of echocardiography-data**

	Pre-engraftment				Post-engraftment			
	Sham	c-ECT	g-ECT	NCM	Sham	c-ECT	g-ECT	NCM
LVEDD (cm)	0.89±0.03	0.89±0.04	0.89±0.05	0.89±0.03	0.99±0.02***	0.89±0.03	0.96±0.04***	0.96±0.03***
LVESD (cm)	0.72±0.02	0.73±0.05	0.74±0.04	0.73±0.04	0.83±0.02***	0.70±0.03*	0.78±0.04***	0.78±0.03***
FS%	17.8±2.6	18.0±2.7	18.0±2.1	17.5±1.7	15.3±1.6***	21.9±2.6***	18.8±2.1*	18.5±2.5
EF%	41.5±5.0	41.9±5.4	39.6±4.4	42.0±4.1	36.3±3.4***	49.1±4.6**	43.4±3.9*	42.8±4.8

Abbreviations: LVEDD, left ventricular end-diastolic dimension; LVESD, left ventricular end-systole dimension; FS, fractional shortening; EF, ejection fraction; NCM, non-cardiomyocytes grafts. Data are mean ± s.e.m. \*=  $p < 0.05$ , \*\*=  $p < 0.01$ , \*\*\*=  $p < 0.001$ . vs. pre-engraftment (paired two-tailed Student *t*-tests).

**Supplementary table 3: Summary of catheterization-data**

	4 weeks after implantation			
	Sham	c-ECT	g-ECT	NCM
LVEDP (mmHg)	16.2 ± 1.1	8.0 ± 0.9 <sup>#</sup>	13.8 ± 1.0 <sup>#§</sup>	14.6 ± 1.0 <sup>#§</sup>
LVESP (mmHg)	89.1 ± 3.4	85.2 ± 2.9 <sup>#</sup>	89.3 ± 3.1	91.3 ± 3.2
Max $dP/dt$ (mmHg/s)	3459.3 ± 83.3	3738.3 ± 87.1 <sup>#</sup>	3553.6 ± 95.8 <sup>#§</sup>	3502.6 ± 60.9 <sup>#§</sup>
Min $dP/dt$ (mmHg/s)	-3176.3 ± 81.3	-3432.1 ± 67.7 <sup>#</sup>	-3286.0 ± 53.2 <sup>#§</sup>	-3246.4 ± 85.3 <sup>#§</sup>

Abbreviations: LVEDP, left ventricular end-diastolic pressure;  $dP/dt$ , change in pressure/ change in time; NCM, non-cardiomyocytes grafts. Data are mean ± s.e.m. <sup>#</sup>

$p < 0.001$ . vs. sham. <sup>§</sup>  $p < 0.001$  vs. c-ECTs (ANOVA with Tukey's test).

## Supplementary Movies

**Supplementary Movie 1.** Three dimensional live cell imaging of c-ECTs at day 8.

**Supplementary Movie 2.** Light microscope of synchronously contracted c-ECTs at day 8.

**Supplementary Movie 3.** Intracellular calcium transient measurement of c-ECTs under spontaneous condition.

**Supplementary Movie 4.** Intracellular calcium transient measurement of c-ECTs under point stimulation condition.

## **Supplementary Methods**

### **Scanning electron microscopy (SEM) analysis**

Hydrogels were dried through a freeze-drying procedure, stored in a desiccator (4-A molecular sieves, EM Science, Gibbstown, NJ), sputter-coated with gold (Autoconductavac IV, See-Vac) for approximately 3 min to a thickness of approximately 20–30 nm, and imaged using scanning electron microscopy at 10 kV.

### **Mechanical Testing**

Compressive modulus of hydrogels was tested by TA.XT2i Texture Analyzer (Texture Technologies Corp.). The test speed was set at 0.1 mm/second. The compressive modulus ( $E_c$ ) was determined on from the slope in the linear region corresponding to 5-15% strain. The shear modulus of hydrogels was obtained from an Advanced Rheology (TA Instruments) rheometer at room temperature.

### **Electrical measurements**

Electrical conductivity of SWNT/gelatin scaffolds and pure gelatin gel was evaluated using a HP 34401A multimeter and probe as well. Two probes were touched the sample surfaces and electrical resistance of the samples was measured dry at room temperature. Each sample was taken for three times.

### **Cell viability assays**

Cardiac cell viability was determined using LIVE/DEAD Viability/Cytotoxicity Kit (Molecular Probes, Invitrogen, Grand Island, NY). At the 1d and 3d of cultivation period, cardiac cells grown within the SWNTs/gelatin hydrogels with different concentration of SWNTs (0, 0.5, 1, 1.5, 2 and 2.5mg/ml) were incubated with 2  $\mu$ M



calcein AM and 4  $\mu$ M EthD-1 in PBS. The number of live and dead cells in 10 randomly selected fields of each group was analyzed by ImageJ software.

### **Construction of g-ECTs and Non-cardiomyocytes grafts**

Ventricular cardiac cells were isolated from 1-day-old neonatal Sprague-Dawley rats and seeded gelatin scaffolds into construct g-ECT ( $7 \times 10^7$  cells/cm<sup>3</sup>). The g-ECTs were cultured under static conditions for 3 days, following 5 days' electrical field stimulation. g-ECTs were transferred into a chamber fitted with two 1/4-inch-diameter carbon rods (Ladd Research Industries, Burlington, VT) placed 1 cm apart and connected to a cardiac stimulator (Nihon Kohden, Tokyo) with platinum wires (Ladd Research Industries). The cell constructs were cultivated in a cell incubator (37°C, 5% CO<sub>2</sub>), under electrical stimulation (rectangular, 2ms pulse, 5 V, 5 V/cm, 1 Hz). Non-cardiomyocytes were derived after plating of freshly isolated neonatal rat heart cells for 1 h. The attached non-cardiomyocytes were cultured and passage at least 3 times to eliminate contaminating cardiac cardiomyocytes. The non-cardiomyocytes ( $7 \times 10^7$  cells/cm<sup>3</sup>) were seeded into SWNT/gelatin scaffolds to construct non-cardiomyocytes grafts (NCM).

### **Cardiac patch labeling and 3-D live cell imaging**

To observe the distribution of cardiac cells in the scaffold, cardiac cell constructs were labeled with 2  $\mu$ g/mL CM-DiI (Molecular Probes, Eugene, OR) at 3d and 8d and were incubated in single-well chambered cover glass tissue culture dishes (NalgeNunc International) and imaged via confocal microscopy (Nikon Eclipse Ti-E) with a Perkin-Elmer Ultra view spinning-disc scanner unit. Cardiac cells constructs were

sequentially scanned every 1  $\mu\text{m}$  space from the surface and 3D cell imaging was analyzed using Volocity software.

### **Histology and immunofluorescence *in vitro*.**

After the cultivation of 3d and 8d, cardiac cellular constructs were fixed in 4% formaldehyde in phosphate buffered saline (PBS) and embedded in paraffin. The sections (4  $\mu\text{m}$ ) were cut and stained with H&E. For immunofluorescence staining, sections were immunolabeled with anti-troponin I antibodies (AbCam, Cambridge MA), connexin43 antibodies (AbCam, Cambridge MA),  $\alpha$ -sarcomeric actinin antibodies (AbCam, Cambridge MA), vimentin (Invitrogen Corp., Carlsbad, CA),  $\alpha$ -SMA (alpha-smooth muscle actin, AbCam, Cambridge MA) and vWF (Invitrogen Corp., Carlsbad, CA) with appropriate secondary antibodies and were counterstained with DAPI (Sigma, USA). Confocal images were viewed by Zeiss LSM 510 microscope.

### **Transmission electron microscopy analysis**

Cardiac cell constructs were fixed in 2.5% glutaraldehyde in 0.1 M sodium cacodylate and then were post-fixed in 1.0% osmium tetroxide in 0.1 M sodium phosphate buffer. After an overnight wash in PBS at 4°C, the constructs were dehydrated through graded ethanol solutions and embedded with Epon 812 according to standard protocols. Ultrathin thin sections were mounted on copper grids and then examined on a Zeiss Leo 906 transmission electron microscope.

### **Western blot analysis *in vitro***

Cardiac cell constructs were solubilized and total proteins (100 $\mu\text{g}$ ) were

electrophoresed by SDS–PAGE and detected by the incubation with antibodies against connexin 43 (Abcam, Cambridge, MA),  $\alpha$ -sarcomeric actinin (Abcam, Cambridge, MA). As control, the expression of GAPDH (Santa Cruz Biotechnology, Santa Cruz, CA) was evaluated. At least three samples were tested with each antibody. The analysis of band intensities was performed with Quantity One software (Bio-Rad).

### **Intracellular calcium transient measurement**

Cardiac cell constructs ( $n \geq 3$  from each group, from three separate experiments) were incubated with 10mM fluo-4 AM (Invitrogen) and 0.1% Pluronic F-127 for 45 min at 37°C and washed three times in modified Tyrode solution. Cell constructs were electrically stimulated at a frequency of 1-2 Hz by a two platinum electrode insert connected to a bipolar stimulator. Videos of the calcium ion staining were acquired using 10 $\times$  0.45 NA objective lens at 12 frame/s 256  $\times$  256 pixels on a Nikon Eclipse Ti-E confocal microscope with a Perkin-Elmer Ultra view spinning-disc scanner unit. Fluo-4 was excited at 488nm and emitted fluorescence (F) was filtered by a 505nm bandpass filter. The images were acquired and subsequently analyzed with the use of Volocity software, and fluorescence signals were normalized to basal cell fluorescence after fluo-4 loading ( $F_0$ ).

### **Histology and immunofluorescence *in vivo*.**

One week and four weeks after patch implantation, hearts were obtained and fixed in 4% formaldehyde in PBS and were performed by morphological analysis. Paraffin-embedded slices (4  $\mu$ m) were stained with hematoxylin-eosin. For

immunofluorescence, we used anti-troponin I (AbCam, Cambridge MA), connexin43 (AbCam, Cambridge MA),  $\alpha$ -sarcomericactinin (AbCam, Cambridge MA), PCNA (AbCam, Cambridge MA),  $\alpha$ -smooth muscle A (AbCam, Cambridge MA), vWF (AbCam, Cambridge MA), and CD68 antibodies (Invitrogen, Carlsbad, CA) as the first antibody and alexa488-conjugated appropriate secondary antibodies (Invitrogen Corp., Carlsbad, CA). Sections were counterstained with DAPI (Sigma, USA). Finally, confocal images were acquired with Zeiss LSM 510 microscope.

### **Echocardiography**

Left ventricular (LV) function was evaluated by a commercially available echocardiography system (Sequoia 512; Acuson) equipped with 14-MHz phased-array transducer. M-mode images were obtained close to the papillary muscle level using the short-axis views. The ventricular end-diastolic dimension (LVEDD) and ventricular end-systole dimension (LVESD), fractional shortening (FS) and EF (ejection fraction) were measured. All measurements were averages of three consecutive cardiac cycles and were made by an experienced technician who was blinded to the treatment group. The left ventricular was obtained from the parasternal long-axis view. For each data point, 3 consecutive cardiac cycles were averaged.

### **Left ventricular catheterization**

Four weeks after patch implantation, hemodynamic evaluation was performed with a fluid-filled catheter. The left ventricular end diastolic pressure (LVEDP), left ventricular end systole pressure (LVESP), max  $dP/dt$  (change in pressure/ change in

time) and  $\min dP/dt$  were obtained by computer recording and monitoring continuously. Data from three consecutive cardiac cycles were statistically analyzed.

### **Western blot analysis *in vivo***

Immunoblotting analyses were conducted as above described. Four weeks after patch implantation, the hearts were harvested and the left ventricular containing the ischaemic zones were solubilized. Rabbit polyclonal anti-connexin 43 antibody, mouse monoclonal anti N-cadherin antibody, rabbit polyclonal anti-Nav1.5 antibody, rabbit polyclonal anti- $\beta$ 1-integrin antibody (all from Abcam, Cambridge, MA), rabbit polyclonal anti-ILK antibody, rabbit polyclonal anti-Akt antibody, mouse monoclonal anti-phospho-Akt (Ser473) antibody, mouse monoclonal  $\beta$ -catenin antibody (all from Cell Signaling Technology) were used.. As control, the expression of GAPDH (Santa Cruz Biotechnology, Santa Cruz, CA) was evaluated. At least three separate samples were tested with each antibody.